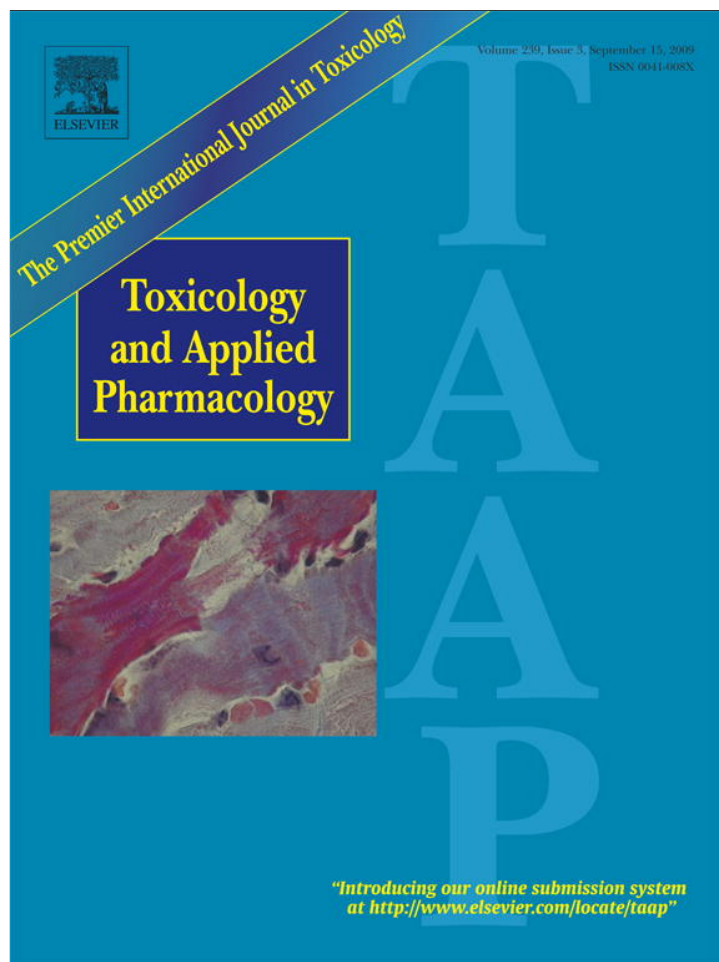


Provided for non-commercial research and education use.
Not for reproduction, distribution or commercial use.



This article appeared in a journal published by Elsevier. The attached copy is furnished to the author for internal non-commercial research and education use, including for instruction at the authors institution and sharing with colleagues.

Other uses, including reproduction and distribution, or selling or licensing copies, or posting to personal, institutional or third party websites are prohibited.

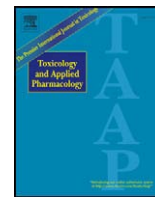
In most cases authors are permitted to post their version of the article (e.g. in Word or Tex form) to their personal website or institutional repository. Authors requiring further information regarding Elsevier's archiving and manuscript policies are encouraged to visit:

<http://www.elsevier.com/copyright>



Contents lists available at ScienceDirect

Toxicology and Applied Pharmacology

journal homepage: www.elsevier.com/locate/ymtaap

Low doses of ochratoxin A upregulate the protein expression of organic anion transporters Oat1, Oat2, Oat3 and Oat5 in rat kidney cortex

Vilim Žlender^a, Davorka Breljak^b, Marija Ljubojević^b, Dubravka Flajs^a, Daniela Balen^b, Hrvoje Brzica^b, Ana-Marija Domijan^a, Maja Peraica^a, Radovan Fuchs^a, Naohiko Anzai^c, Ivan Sabolić^{b,*}

^a Unit of Toxicology, Institute for Medical Research and Occupational Health, Zagreb, Croatia

^b Molecular Toxicology, Institute for Medical Research and Occupational Health, Ksaverska cesta 2, HR-10001, Zagreb, Croatia

^c Department of Pharmacology and Toxicology, Kyorin University School of Medicine, Tokyo, Japan

ARTICLE INFO

Article history:

Received 5 February 2009

Revised 22 May 2009

Accepted 8 June 2009

Available online 16 June 2009

Keywords:

Kidney
Membrane transporters
Mycotoxins
Nephrotoxicity
Organic anions
PAH
Proximal tubule

ABSTRACT

Mycotoxin ochratoxin A (OTA) is nephrotoxic in various animal species. In rodents, OTA intoxication impairs various proximal tubule (PT) functions, including secretion of *p*-aminohippurate (PAH), possibly via affecting the renal organic anion (OA) transporters (Oat). However, an effect of OTA on the activity/expression of specific Oats in the mammalian kidney has not been reported. In this work, male rats were gavaged various doses of OTA every 2nd day for 10 days, and in their kidneys we studied: tubule integrity by microscopy, abundance of basolateral (rOat1, rOat3) and brush-border (rOat2, rOat5) rOat proteins by immunohistochemical methods, and expression of rOats mRNA by RT-PCR. The OTA treatment caused: a) dose-dependent damage of the cells in S3 segments of medullary rays, b) dual effect upon rOats in PT: low doses (50–250 µg OTA/kg b.m.) upregulated the abundance of all rOats, while a high dose (500 µg OTA/kg b.m.) downregulated the abundance of rOat1, and c) unchanged mRNA expression for all rOats at low OTA doses, and its downregulation at high OTA dose. Changes in the expression of renal Oats were associated with enhanced OTA accumulation in tissue and excretion in urine, whereas the indicators of oxidative stress either remained unchanged (malondialdehyde, glutathione, 8-hydroxydeoxyguanosine) or became deranged (microtubules). While OTA accumulation and downregulation of rOats in the kidney are consistent with the previously reported impaired renal PAH secretion in rodents intoxicated with high OTA doses, the post-transcriptional upregulation of Oats at low OTA doses may contribute to OTA accumulation and development of nephrotoxicity.

© 2009 Elsevier Inc. All rights reserved.

Introduction

Ochratoxin A (OTA) is ubiquitous fungal metabolite and food contaminant with nephrotoxic and carcinogenic potential in animals and humans (EFSA, 2006; Kuiper-Goodman and Scott, 1989; Pfohl-Leschkowicz and Manderville, 2007). It has been shown in various animal models (rat, pig, chicken) that OTA: a) accumulates largely in the proximal tubule (PT) cells, b) induces dose- and time-dependent impairment of PT function, resulting in limited polyuria, glucosuria, proteinuria and enzymuria, and diminished secretion of organic anions (OA), c) damages the renal structure, manifested by tubule degeneration, apoptosis, necrosis, and exfoliation of PT cells, predominantly involving the pars recta segment (S3), and d) causes focal tubular proliferative effects, including cell hyperplasia and tubular cell adenoma and carcinoma (Boorman et al., 1992; Castegnaro et al., 1998; Kuiper-Goodman and Scott, 1989; Kumar et al., 2007; Lee et al., 1984; Rached et al., 2007; Sauvante et al., 2005).

In some studies, usually after treating experimental animals with OTA for a few months or years, cellular mechanisms of OTA toxicity were associated with increased lipid peroxidation and formation of malondialdehyde (MDA), DNA damage, and apoptosis, and were counteracted by the scavengers of reactive oxygen species (ROS), thus indicating oxidative stress as a possible mediator of toxicity (Cavin et al., 2007; Grosse et al., 1997; Kamp et al., 2005; Petrik et al., 2003; Ringot et al., 2006; Schaaf et al., 2002).

OTA has a long plasma half life in the body, mainly due to binding to serum proteins, slow biotransformation, entero-hepatic circulation, and reabsorption in kidney (Fuchs and Hult, 1992). The renal excretion of OTA via glomerular filtration is limited, and largely proceeds via transepithelial secretion in PT (Bahnmann et al., 1997; Jung et al., 2001; Welborn et al., 1998). The filtered and/or secreted OTA is partially reabsorbed along the nephron, mostly in the PT S3 segments (Dahlmann et al., 1998; Zingerle et al., 1997). Filtration and transepithelial secretion, followed by reabsorption, represent an effective way of OTA accumulation in kidneys and may be a base for development of nephrotoxicity. OTA itself is an OA and a substrate of various renal OA transporters (Oat) located in the basolateral (BLM) or

* Corresponding author. Fax: +385 1 4673 303.
E-mail address: sabolic@imi.hr (I. Sabolić).

luminal membrane domain of (mainly) PT cells. In the mammalian kidney, OTA can be transported by Oat1 (*Slc22a6*), Oat2 (*Slc22a7*), Oat3 (*Slc22a8*), OAT4 (*SLC22A11*; absent in rodents), Oat5 (*Slc22a19*; absent in humans), Oat-K1 (*Oatp1a3/Slco1a3*), H⁺-dipeptide cotransporter (PEPT/family *Slc15*), and ATP-driven multidrug resistance-associated protein Mrp2 (*Abcc2*) (Anzai et al., 2005; Babu et al., 2002; Cha et al., 2001; Enomoto et al., 2002; Kobayashi et al., 2002; Kusuhara et al., 1999; Kwak et al., 2005; Leier et al., 2000; Takeuchi et al., 2001; Tsuda et al., 1999; Youngblood and Sweet, 2004). In the rodent PT, Oat1 and Oat3 are localized in the BLM and thus may mediate internalization of OTA at the basolateral side. Oat2, Oat5, Oat-K1, and PEPT are localized in the brush-border membrane (BBM) and thus may mediate reabsorption of OTA, whereas Mrp2 in the BBM may serve as an active extruder of OTA.

Earlier studies in various experimental models indicated that OTA, being itself a substrate for various Oats, can interact with the transport of other OA. In these studies: a) OTA directly and competitively inhibited the basolateral transport of a prototypical OA *p*-aminohippurate (PAH) in isolated PT segments and renal cortical membranes, b) in the presence of OTA, the accumulation of PAH in the renal cortical slices, isolated PT cells, and PT-derived established cell lines, was impaired, and c) the OTA-treated experimental animals exhibited a diminished accumulation of PAH in the renal cortical slices *in vitro* and a lower PAH clearance *in vivo* (Friis et al., 1988; Gekle and Silbernagl, 1994; Groves et al., 1998, 1999; Jung et al., 2001; Sauvant et al., 1998; Sokol et al., 1988; Welborn et al., 1998). These data thus indicated that OTA may affect the activity and/or expression of renal Oats, but such possibilities have not been experimentally verified. In order to test if OTA affects the cellular expression and distribution of renal Oats, here we used an *in vivo* model of OTA intoxication in adult male rats, and characterized the protein and mRNA expression levels of the two basolateral (Oat1, Oat3) and two brush-border (Oat2, Oat5) OA/OTA transporters in PT. The Oat data were correlated with the tissue morphology, OTA accumulation in the renal tissue and its excretion in urine, and with the tissue and/or urine indicators of oxidative stress.

Materials and methods

Animals and treatment. Adult (12–14 weeks old) male Wistar rats were from the breeding colony at the Institute in Zagreb. Animals were bred and maintained according to the Guide for Care and Use of Laboratory Animals (National Institute of Health, Bethesda, USA, 1996). The studies were approved by the Institutional Ethics Committee.

OTA was dissolved in 51 mM NaHCO₃, pH 7.4, and given by gastric gavage. Animals (4 rats/experimental group) were gavaged with various OTA doses (50, 125, 250 and 500 µg/kg b.m.) every 2nd day for 10 days (in total, 5 doses; the last gavage was given on the 9th day, e.g., the day before termination). Control rats were gavaged an equivalent volume of solvent (10 ml/kg b.m.), using the same time pattern. The gavage was executed between 8 and 9 am.

Antibodies. The use of affinity purified, rabbit-raised anti-peptide polyclonal antibodies against the rat OA transporter (rOat) proteins rOat1 (rOat1-ab), rOat2 (rOat2-ab), rOat3 (rOat3-ab), and rOat5 (rOat5-ab) in immunoblotting and immunocytochemical studies was described in details elsewhere (Anzai et al., 2005; Ljubojevic et al., 2004, 2007). Monoclonal antibodies against α -actin (actin-ab) and α -tubulin (tubulin-ab) were purchased from Chemicon Int. (Temecula, CA, USA) and Sigma (St. Louis, MO, USA), respectively. Secondary antibodies, e.g., the CY3- (GARCY3) or alkaline phosphatase-labeled (GARAP) goat anti-rabbit IgG, CY3-labeled donkey anti-mouse IgG (DAMCY3), and alkaline phosphatase-labeled goat anti-mouse IgG (GAMP) were purchased from Jackson ImmunoResearch Laboratories, Inc. (West Grove, PA, USA) or Kirkegaard and Perry (Geithersburg, MD, USA).

Chemicals. Anesthetics (Narketan and Xylapan) were purchased from Chassot AG (Bern, Switzerland). OTA (free acid; 99% purity; Cat. No. O1877), protease inhibitors (phenyl-methyl-sulfonyl-fluoride (PMSF), antipain, benzamidin), 1,1,3,3-tetramethoxy propane, butylated hydroxytoluene, and 2-thiobarbituric acid (TBA) were purchased from Sigma (St. Louis, MO, USA). Water and silica gel Si-60 (15–40 µm) for HPLC studies were obtained from Merck (Darmstadt, Germany). Other chemicals and reagents were the analytical or molecular biology grade, and their commercial source was either Kemika (Zagreb, Croatia) or is indicated under description of specific methods.

Determination of urine biochemical parameters. On the 9th day of treatment, rats were gavaged with the last (5th) dose of OTA or vehicle (controls), placed individually in the metabolic cages, deprived of food but with free access to water, and urine was collected for 24 h. The final urine volume was measured, an aliquot was centrifuged at 2500 ×g for 15 min to remove the particulate debris, and analysis of various parameters (glucose, creatinine, inorganic phosphate, potassium, chloride, sodium) was performed in the supernatant using the biochemical analyzer Olympus AU 600 (Tokyo, Japan) and HPLC apparatus (Shimadzu Corporation, Kyoto, Japan) and commercial substrates. Protein was measured by the dye-binding method (Bradford, 1976).

OTA analysis. Before determination, OTA was extracted from urine and the kidney and liver tissues. OTA in urine was extracted by the method of Breitholtz-Emanuelsson et al. (1993). Kidneys and livers were collected from the animals terminated by cervical dislocation, washed in physiological saline (0.9% NaCl), the respective renal (pooled cortex plus outer stripe) and liver (the largest lobe) tissues were manually separated, weighed, and kept frozen at –20°C until further analysis. A 10% homogenate of the thawed tissues was prepared in saline, and OTA was extracted exactly as described by Bauer von et al., 1984.

The extracted OTA was determined by HPLC. The HPLC apparatus consisted of degasser, isocratic pump, the column oven (Shimadzu Corporation, Kyoto, Japan), and the fluorescent detector (Thermo Separation Products – Spectra System FL 2000, Fremont, CA, USA). The guard column (4.0 × 4.0 mm) and the analytical column (4.0 × 125.0 mm) were C-18 reverse-phase (LiChrospher, Merck, Darmstadt, Germany) with 5 µm particles. The mobile phase, consisting of methanol, water and acetic acid (700:300:20, v/v), was degassed before use in an ultrasonic bath for 15 min. The flow-rate was 0.5 mL min⁻¹. The excitation and emission wavelengths were 336 nm and 464 nm, respectively. The injection volume was 20 µL and the temperature in the column oven was set at 32°C. Under these conditions, the retention time of OTA was about 8 min.

OTA concentration in tissue homogenates and urine samples was calculated from the integrated peak area and linear regression curve obtained with OTA standards. In preliminary experiments, the peak areas of the standards were found to be linear with 0.1–15 ng OTA/mL (not shown). The OTA standards were prepared by adding known amounts of stock solution of OTA to portions of OTA-free urine and control (OTA-untreated) kidney and liver tissue homogenates before the extraction. The concentration of OTA stock solution was checked spectrophotometrically at 333 nm using 6640 M⁻¹ cm⁻¹ as the extinction coefficient.

Determination of malondialdehyde (MDA) and 8-hydroxydeoxyguanosine (8-OHdG). To determine a lipid peroxidation product MDA, urine samples were processed by the method of Drury et al. (1997), whereas the renal (cortex plus outer stripe) and liver homogenates were processed by the method of Ohkawa et al. (1979).

MDA was measured by HPLC, using the columns described above for OTA. The mobile phase (50 mM KH₂PO₄ and methanol (60:40, v/v),

pH 6.8) was degassed before use in the ultrasonic bath for 15 min. The flow-rate was 1 mL min⁻¹, and the UV detector was set at 532 nm. The injection volume was 20 µL, and temperature in the column oven was set at 32°C. Under these conditions, the retention time of MDA was about 2.5 min. Quantification of MDA in tissue homogenates and urine was performed by comparing the peak area with the regression curve for MDA standards in aqueous solution, which was linear in the range of 0.3–15 µmol/L (not shown).

8-OHdG, an oxidative DNA adduct, was determined only in the urine by HPLC, as described in detail in our recent publication (Domijan and Peraica, 2008). Quantification of 8-OHdG in urine was performed from the measured peak area using the regression curve for aqueous standard solution, which was linear in the range of 50–400 nmol/L (not shown).

Tissue fixation, immunofluorescence staining, and tissue morphology.

In anesthetized rats the circulatory system was perfused *in vivo* via the left ventricle of the heart with aerated (95% O₂/5% CO₂) and temperature-equilibrated (37°C) phosphate-buffered saline (PBS; in mM: 137 NaCl, 2.7 KCl, 8 Na₂HPO₄, 2 K₂PO₄, pH 7.4) for 2–3 min. The left kidney was then ligated and removed for preparation of tissue homogenates and RNA isolation (*vide infra*). The right kidney was further perfused with 150 ml of fixative (4% *p*-formaldehyde). Further handling of the tissues, cutting of 4-µm thick tissue cryosections, rOat- and α-tubulin-specific retrieval steps to reveal the cryptic antibody binding sites, blocking with albumin solution, as well as incubation with optimal dilutions of primary and secondary antibodies were described in detail elsewhere (Ljubojevic et al., 2004, 2007; Sabolic et al., 2006).

The stained sections were examined with an Opton III RS fluorescence microscope (Opton Feintechnik, Oberkochen, Germany) and photographed using a Spot RT Slider digital camera and software (Diagnostic Instruments, Sterling Heights, MI, USA). The photos were imported into Adobe Photoshop 6.0 for processing and labeling. The CY3-related immunostaining was inspected under the specific filter for red fluorescence, whereas the tissue autofluorescence under the filter for green fluorescence was used to monitor morphology of the tubules in non-stained or CY3-stained sections. Where required, the Adobe Photoshop software was later used to convert red or green fluorescence into black and white mode.

Preparation of tissue homogenates and membranes for PAGE. The removed left kidney was decapsulated and either used *in toto* or sagittally sliced, and the pooled tissue (cortex plus outer stripe) was dissected manually. The tissue was homogenized (10% homogenate) in a chilled buffer (in mM: 300 mannitol, 5 EGTA, 12 Tris-HCl, pH 7.4, 1 PMSF, 0.1 benzamide, and 0.1 µg/mL antipain) with a Powergen-125 homogenizer (Fisher Scientific, New Jersey, NJ, USA) at the maximal setting (1 min homogenization–2 min pause–1 min homogenization). Total cell membranes (TCM) were isolated from tissue homogenates by differential centrifugation using refrigerated centrifuges. The cell debris was first removed by centrifugation at 6000 ×g for 15 min, and the supernatant was centrifuged at 150,000 ×g for 1 h. The resulting pellet (TCM) was resuspended in a chilled buffer (150 mM mannitol, 2.5 mM EGTA, 6 mM Tris-HCl, pH 7.4). The protein was determined by the dye-binding assay (Bradford, 1976), adjusted to the desired concentration, and the membranes were stored at –70°C until further use.

SDS-PAGE and Western blotting. Following the optimal conditions for SDS-PAGE and Western blotting of various rOats in isolated renal membranes (Ljubojevic et al., 2004, 2007), frozen TCM were thawed at 37°C, mixed with Laemmli buffer (final: 1% SDS, 12% glycerol, 30 mM Tris-HCl, pH 6.8), and heated in nondenaturing conditions (without SH-reagents) at 65°C for 15 min. Protein separation through 10% SDS-PAGE, electrophoretic transfer to Immobilon (Millipore,

Bedford, MA, USA), incubation of this membrane in blotting-buffer (5% non-fat dry milk, 0.15 M NaCl, 1% Triton X-100, 20 mM Tris-HCl, pH 7.4) without or with the optimal concentrations of primary and secondary antibodies, as well as visualization of the labeled protein bands with the alkaline phosphatase activity-mediated reaction, were described in detail in our recent publications (Ljubojevic et al., 2004, 2007). Intensity of the labeled protein bands was scanned and expressed in arbitrary units, relative to the strongest band (=1 arbitrary unit) in control samples.

Isolation of RNA and synthesis of first-strand cDNA. The unfixed kidney was removed, decapsulated, cut into ~2 mm thick sagittal slices, and one (middle) slice was immediately submerged into the RNAlater solution (Sigma, St. Louis, MO, USA). The pooled tissue (cortex plus outer stripe) was later dissected manually and used in further isolation steps. Total cellular RNA was extracted using Trizol (Invitrogen) according to manufacturer's conditions. RNA concentration and its purity were estimated by measuring the optical density at 260 and 280 nm. The quality and integrity of RNA were verified by agarose gel electrophoresis. Isolated RNAs were stored at –70°C and subsequently used for RT-PCR studies.

First-strand cDNA synthesis was performed using the First Strand cDNA Synthesis Kit (Fermentas Int., Ontario, Canada) following the manufacturer's instructions. Total cellular RNA (3 µg) was denatured at 70°C for 5 min in the reaction mixture containing 0.5 µg oligo dT (18) and reversed transcribed in total volume of 20 µL reaction mixture containing 1× reverse transcription buffer, 20 U of ribonuclease inhibitor, 1 mM of dNTP mix, and 40 U of Moloney murine leukemia virus reverse transcriptase. The reaction mixture was incubated at 37°C for 60 min followed by incubation at 72°C for 10 min. cDNAs were diluted 5× in DNase/RNase free water (Gibco-BRL, Grand Island, NY, USA) and stored at –20°C until use.

End-point RT-PCR. PCR was performed in total volume of 20 µL using: 1 µL of 5× diluted first-strand cDNA, 0.4 µM specific primers and ready to use PCR Master Mix (Fermentas Int., Ontario, Canada) following instructions by the manufacturer. To avoid amplification of genomic DNA, intron over-spanning primers were used. Custom primers for rOats and GAPDH were purchased from Invitrogen. Forward and reverse sequences of these primers are listed in Table 1. Reaction conditions used for PCR were: initial denaturation for 3 min at 94°C, denaturation for 30 s at 95°C, annealing for 30 s at 57°C, and elongation for 45 s at 72°C. RT-PCR products were resolved by electrophoresis in 1% agarose gel stained with ethidium bromide, and visualized under ultraviolet light. The housekeeping gene GAPDH was used as a control for variations in the input of RNA. To obtain quantitative results, preliminary experiments were done to determine the optimal number of the PCR cycles within the exponential phase of the PCR reaction. The resulting optimal number of cycles was: 25 for rOat1, 32 for rOat2, 26 for rOat3 and rOat5, and 21 for GAPDH.

Table 1
Primer sequences used for end-point RT-PCR.

Gene	Forward and reverse primers (5'–3')	Gene bank accession no.	Location	RT-PCR product size, bp
rOat1	F: GGCACCTTGATTGGCTATGT R: CCACAGCATGGAGAGACAGA	NM_017224.2	712–731 1064–1083	372
rOat2	F: CGCTCAGAATTCTCTCCAC R: ACATCCAGCCTCAACT	NM_053537.2	374–393 665–684	311
rOat3	F: CGGAATAGCCAACCACAAC R: ATCACAGGTCCTCAACCAG	NM_031332.1	210–229 523–542	333
rOat5	F: GGAGGCAGCAGACAAAAC R: TTGCTCTCTAATGATGCC	XM_342011.2	1104–1123 1431–1450	346
GAPDH	F: GGTGATGCTGGTCTGAGTA R: GGATGCAGGGATGATTTCT	NM_017008.3	332–351 681–700	369

Genes: rat orthologs of organic anion transporters and GAPDH. F, forward; R, reverse.

Real-time RT-PCR. Real-time RT-PCR was performed in a 50 μL volume using 3.3 μL (100 ng) of the first-strand cDNA template, 2.5 μL of 20 \times Taqman Gene Expression Assays mix, 25 μL of the 2 \times TaqMan Universal PCR Master Mix (all from Applied Biosystems, Foster City, CA, USA) and 19.2 μL of nuclease-free water. Primers and probes were designed by Applied Biosystems and supplied as Taqman Gene Expression Assays Mix containing a 20 \times mix of unlabeled PCR forward and reverse primers as well as TaqMan MGB probe. Amplification and detection were performed using the 7500 Real-Time PCR System (Applied Biosystems). Thermal cycling

conditions included initial 2 min at 50 $^{\circ}\text{C}$, then 10 min at 95 $^{\circ}\text{C}$, followed by 40 two-step cycles of denaturation (15 s at 95 $^{\circ}\text{C}$) and annealing/extension (1 min at 60 $^{\circ}\text{C}$). To standardize the input of cDNA amount, an endogenous control, i.e., the housekeeping gene β -actin was run, quantified, and the results were normalized to these values. Each sample was performed in duplicate. Relative quantification of rOats mRNA amount (mean fold changes \pm S.E.M of duplicate measurements) was accomplished by comparative Ct-method using the Relative Quantification Study Software (Applied Biosystems).

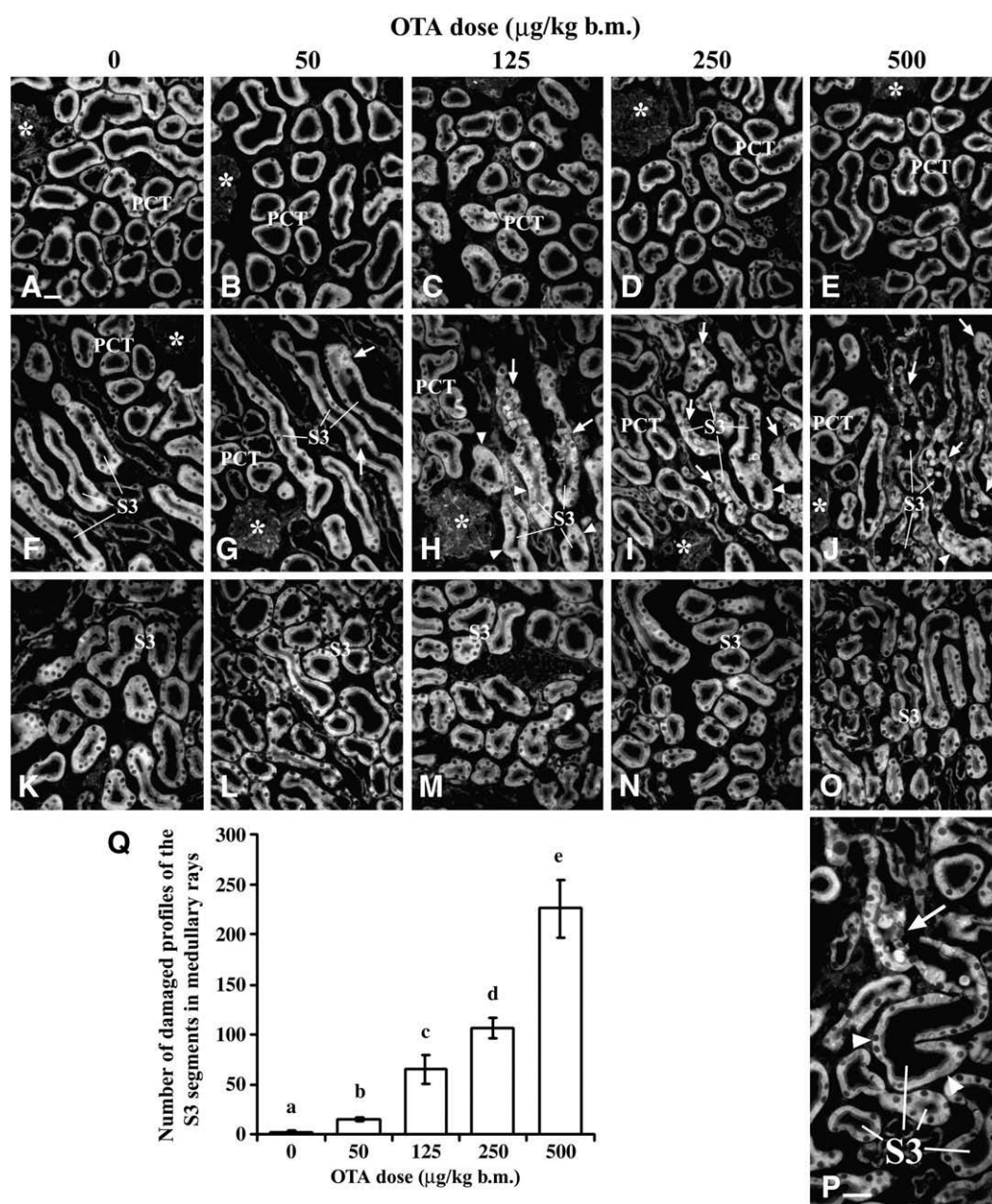


Fig. 1. Morphology of tubules in the superficial cortex (A–E), medullary rays (F–J, P) and outer stripe (K–O) in vehicle (0) and OTA-treated (50–500 μg OTA/kg b.m.) rats. In the superficial cortex (A–E), morphology of glomeruli (asterisks) and various tubules, including the proximal convoluted tubules (PCT), was not visibly affected by OTA treatment. In the medullary rays (I–J, P), the PT S3 segments exhibited the OTA dose-dependent damage; in animals treated with 50 μg OTA/kg b.m., only the individual cells in some S3 profiles were damaged (G, arrows), whereas with higher OTA doses, the damage was more extensive and dose-dependent, exhibiting loss of tubular form, desquamation of BBM and epithelial cells, thinning of epithelium, and accumulation of cell debris in the tubule lumen (H–J, arrows). However, the more distal parts of these profiles at the border with outer stripe were less or not at all affected (H–J, P, arrowheads). In the outer stripe (K–O), the S3 profiles remained unaffected by OTA treatment; the tubule profiles with damaged cells were rare (not shown). Bar = 20 μm . (Q) The number of S3 profiles (mean \pm SEM; $N = 4$ in each experimental group) in the medullary rays, which exhibited a clear damage of epithelium. Damaged S3 profiles were counted in sagittal cryosection from the middle slice of the right kidney from each rat. Statistics (ANOVA): a:b and c:d, N.S.; all other relations, $P < 0.05$. Morphology of the more distal parts of the nephron was visually unchanged by OTA treatment (not shown).

Presentation of the data. The immunocytochemical and Western blotting data represent findings in 4 animals in each experimental group. The end-point and real-time RT-PCR data were obtained with independent cDNA (mRNA) preparations from two control and two OTA-treated animals in each experimental group. RNA for end-point RT-PCR and for real-time RT-PCR were isolated from different animals. The numeric data were expressed as means \pm SE and, where applied, statistically evaluated by using Student's *t*-test or ANOVA with Duncan test at the 5% level of significance.

Results

Reabsorptive functions of renal tubules in OTA-treated rats

In order to determine the OTA-induced renal functional and structural changes, specific urine parameters were analyzed and microscopic examination of the tissue cryosections was performed in rats treated with vehicle or various OTA doses for 10 days. In this initial study, in the 24-h urine from 8 vehicle-treated and 8 OTA-treated (50–500 $\mu\text{g}/\text{kg}$ b.m.) animals we compared the urine volume, glucose, creatinine, phosphate, potassium, chloride, and sodium, and found that these parameters in control and OTA-treated animals were not significantly different (data not shown). Furthermore, the OTA treatment did not induce major change in urine protein (data not shown), except the rats treated with the highest OTA dose exhibited an elevated proteinuria (45.9 ± 2.48 mg protein/24 h), which was, however, not statistically different from that in vehicle-treated animals (27.8 ± 8.39 mg protein/24 h). These data thus indicated that, overall, the 10-day treatment of rats with up to 500 μg OTA/kg b.m. did not cause major loss of reabsorptive kidney functions.

Morphology of renal tubules in OTA-treated rats

The study of tissue morphology revealed the OTA dose-dependent damage of PT S3 segments, predominantly in the medullary rays (Fig. 1). Whereas the proximal convoluted tubules (S1/S2 segments) and other tubule profiles in the kidney cortex were not affected by any OTA dose (A–E), S3 segments in the medullary rays exhibited an OTA dose-dependent damage, which was manifested by variable loss of regular tubular structure and cell membrane, desquamation of the luminal membrane and whole cells, thinning of epithelium, and accumulation of the cell debris in the tubule lumen (F–J). In controls (F), and more at 50 μg OTA/kg b.m. (G), only the individual cells in some S3 were damaged (arrows). Damage was more extensive at higher OTA doses (H–J, arrows); at 500 μg OTA/kg b.m., practically all S3 profiles in the medullary rays were heavily damaged (J, arrows). The proximal convoluted segments in the vicinity of S3, but outside the medullary rays, showed no signs of damage (G–J, PCT). The number of S3 profiles in the medullary rays, which had at least some cells damaged, was visually counted over the surface of one middle cryosection through the right kidney from each animal; as shown in Fig. 1Q, the number of damaged S3 profiles in the medullary rays increased dramatically with increasing the OTA dose. Damage was more extensive in the proximal parts of S3, whereas the most distal parts of S3 located in the medullary rays (H–J, P; arrowheads), as well as the S3 profiles in the outer stripe (K–O), exhibited only a small (occasional individual cells; not shown) or no visible damage of the epithelium.

Effects of OTA treatment on epithelial morphology in renal tubules was further tested by immunostaining microtubules, one of the cytoskeletal elements known to be sensitive marker of the cell integrity in various conditions associated with oxidative stress induced by hypoxia and heavy metal toxicity (Sabolic, 2006, and references there in). Fig. 2 shows microtubules in various nephron segments localized in the superficial cortex (A–C), medullary rays (D–F), and outer stripe (G–I) of control and OTA-treated rats. In all three

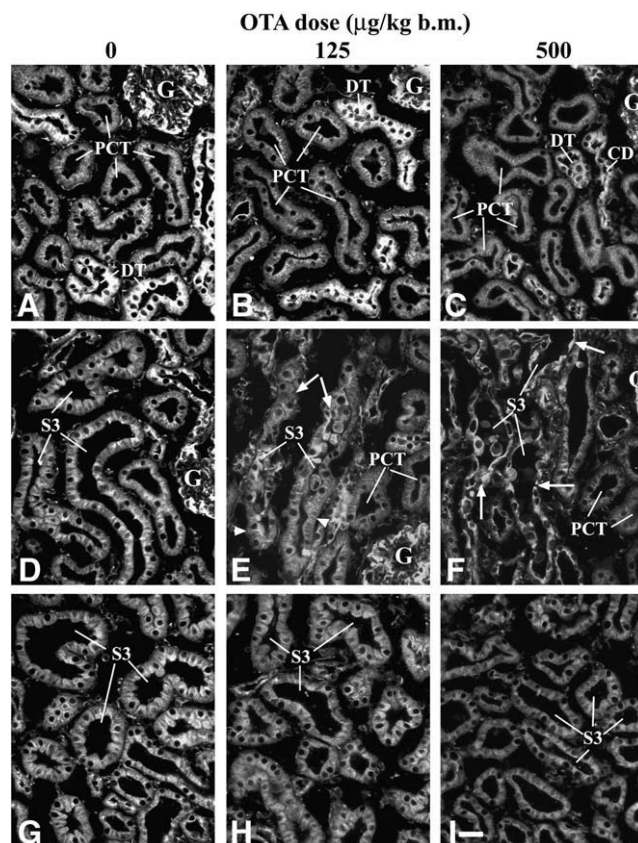


Fig. 2. Immunostaining of microtubules with tubulin-ab in cryosections of the superficial kidney cortex (A–C), medullary rays (D–F) and outer stripe (G–I) from rats treated with vehicle (0) or OTA (125 or 500 $\mu\text{g}/\text{kg}$ b.m.). In vehicle-treated rats (0), microtubules in various tubules were arranged in apico-basally oriented regular bundles, which were more abundant in distal tubules and collecting ducts. Glomeruli (G) were also strongly stained. In rats treated with 125 μg OTA/kg b.m., and even more so in those treated with 500 μg OTA/kg b.m., the staining intensity and the regularity of microtubule bundles were overall diminished in all tissue zones. In the damaged S3 profiles in the medullary rays, microtubules were heavily deranged (E, F; S3, arrows), whereas in the less damaged distal parts of S3, a limited regularity of microtubules was still retained (E, arrowheads). The S3 profiles in the outer stripe (G–I) showed the OTA dose-dependent loss of staining intensity. G, glomeruli; PCT, proximal convoluted tubules; DT, distal tubules; CD, collecting ducts. Bar = 20 μm .

regions in vehicle-treated rats (A, D, G), the strongly stained microtubules in various tubules were assembled in regular, apico-basally oriented bundles of tread-like filaments, which were more abundant in distal tubules and collecting ducts. However, in rats treated with 125 μg OTA/kg b.m. (B, E, H), 250 μg OTA/kg b.m. (data not shown), and 500 μg OTA/kg b.m. (C, F, I), in all three regions we observed the OTA dose-dependent general decrease in staining intensity and deranged microtubule bundles, whereas the damaged S3 profiles in the medullary rays exhibited heavily deranged microtubule network (E, F; arrows).

Cell domain-specific immunolocalization of rOats in the rat nephron

In accordance with our previous immunolocalization studies of Oat1, Oat2, Oat3, and Oat5 with specific polyclonal antibodies in the rat and mouse kidneys (Anzai et al., 2005; Ljubojevic et al., 2004, 2007), in Fig. 3 we confirmed localization of these rOats in the specific cell membrane domains along the rat nephron. The green images showing morphology of various tubule profiles in the kidney cortex (A, B) and outer stripe (C, D) were overlapped with the red immunostaining related to specific rOats in the same tubules. Accordingly, rOat1 was localized to the BLM of PT S2 segments in the cortex (A, strong staining) and S3 segments in the outer stripe

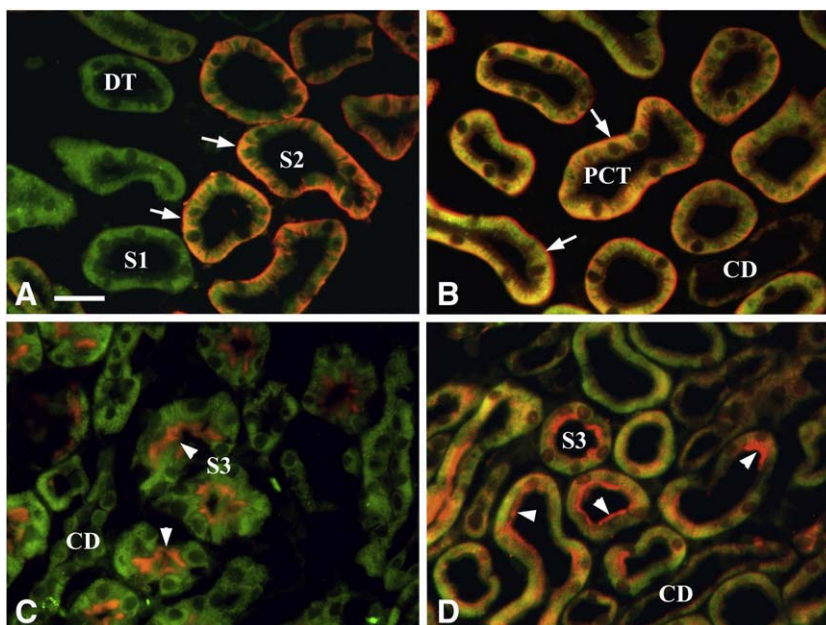


Fig. 3. Cell membrane domain-specific immunolocalization of rOats in various nephron segments of male rats. The images showing morphology of various tubule profiles in the kidney cortex (A, B) and outer stripe (C, D) were taken under the green fluorescent filter. The red, rOat-specific immunostaining in the same tubules was taken separately, and both green and red images were merged in Photoshop. (A) rOat1 was localized to the BLM (arrows) of PT S2 segments in the cortex; the S1 segments and distal tubules (DT) were unstained. The S3 segments in the medullary rays and outer stripe were also weakly stained (not shown). (B) rOat3 was stained with various intensities in the BLM (arrows) of proximal convoluted tubules (PCT), collecting ducts (CD) and other tubules in the cortex. Various nephron segments in other kidney zones were also weakly stained (not shown). (C) rOat2 was weakly stained in the BBM (arrowheads) of PT S3 segments in the outer stripe; the surrounding collecting ducts (CD) were not stained. (D) rOat5 was localized to the BBM (arrowheads) and intracellular organelles of PT S3 segments in the outer stripe; other tubule profiles were negative. Bar = 20 μ m.

(not shown, weak staining), rOat3 was localized to the BLM of various tubules in the cortex (B) and other kidney zones (not shown), rOat2 was localized to the BBM of PT S3 segments in the outer stripe (C), whereas rOat5 was localized to the BBM and intracellular organelles of PT S3 segments in the outer stripe (D).

OTA treatment changed the expression of basolateral OA transporters Oat1 and Oat3

In accordance with our recent studies in the rat kidneys (Ljubojevic et al., 2004, 2007), in immunoblots of TCM from the kidney cortex and outer stripe the rOat1-ab labeled the complex (glycosylation-related) ~68 kDa protein band, whereas the actin-ab labeled the 42 kDa protein band (Fig. 4). The pattern (A) and densitometric evaluation of these bands (B) show that the OTA treatment resulted in a dose-dependent change in rOat1 protein abundance, exhibiting a significant (~50% above controls) increase at 125 μ g OTA/kg b.m. and strong decrease (~70% vs. controls) at 500 μ g OTA/kg b.m. The abundance of α -actin was not affected by OTA. By immunocytochemistry, in control rats the rOat1-ab stained the BLM of PT S2 segments in the cortex (strongly) and S3 segments in the medullary rays and outer stripe (weakly) (C). In OTA-treated rats, the cortical tubules were stained with an increased intensity at lower (50–250 μ g/kg b.m.) and a strongly decreased intensity at the highest (500 μ g/kg b.m.) mycotoxin dose. The S3 segments in the outer stripe only showed a decreased intensity at the highest OTA dose (C). The data of end-point (D) and real-time RT-PCR (E) show that in comparison with controls, the expression of rOat1 mRNA in the renal tissue (pooled cortex and outer stripe) was unchanged at 50–250 μ g OTA/kg b.m., and dramatically decreased (~85%) at the highest OTA dose.

In accordance with previous findings in the rat kidney (Kojima et al., 2002; Ljubojevic et al., 2004), the rOat3-ab in TCM from the renal tissue of control rats labeled the glycosylation-related complex protein band of ~66 kDa (Fig. 5A) and stained the BLM of various tubules in the cortex and outer stripe (C). As shown by the labeled

bands (A), and by densitometric evaluation of these bands (B), in OTA-treated rats the abundance of rOat3 protein in TCM was strongly increased (~200% above the values in controls) at 125–250 μ g OTA/kg b.m., and then leveled off at 500 μ g OTA/kg b.m. The immunostaining data in the kidney cortex corroborated the Western blotting data (C); compared with controls, the staining intensity was strongly enhanced in rats treated with 125–250 μ g OTA/kg b.m., whereas in rats treated with 500 μ g OTA/kg b.m., the staining of cortical tubules was similar to that in controls. In the outer stripe, the staining intensity was unaffected by OTA treatment. The end-point and real-time RT-PCR data showed that the expression of rOat3 mRNA in the renal tissue was largely unaffected in rats treated with 50–250 μ g OTA/kg b.m., and strongly decreased (~40% with respect to controls) at 500 μ g OTA/kg b.m. (D, E).

OTA treatment changed the expression of brush-border OA transporters Oat2 and Oat5

Previous immunochemical studies in adult rats described the rOat2 protein of ~66 kDa in the BBM of PT S3 segments in the outer stripe and medullary rays (Kojima et al., 2002; Ljubojevic et al., 2007). Accordingly, in the kidney samples from control rats the rOat2-ab labeled the 66 kDa protein in TCM (Fig. 6A) and weakly stained the apical domain of S3 in the outer stripe (C). The pattern of protein bands (A) and their densitometric evaluation (B) indicate that the abundance of rOat2 protein in TCM strongly increased (~140% above controls) at 125–250 μ g OTA/kg b.m. and declined to the control levels at 500 μ g OTA/kg b.m. This pattern was confirmed by immunostaining tubules in the outer stripe; in controls, only the occasional tubules were weakly apically positive, in animals treated with 125 (not shown) and 250 μ g OTA/kg b.m. (C), many positive tubules with higher staining intensity were observed, whereas the staining was negligible at 500 μ g OTA/kg b.m. The end-point (D) and real-time (E) RT-PCR data show that the rOat2 mRNA expression was not affected by up to 250 μ g OTA/kg b.m., and strongly decreased (~60% vs. controls) at 500 μ g OTA/kg b.m.

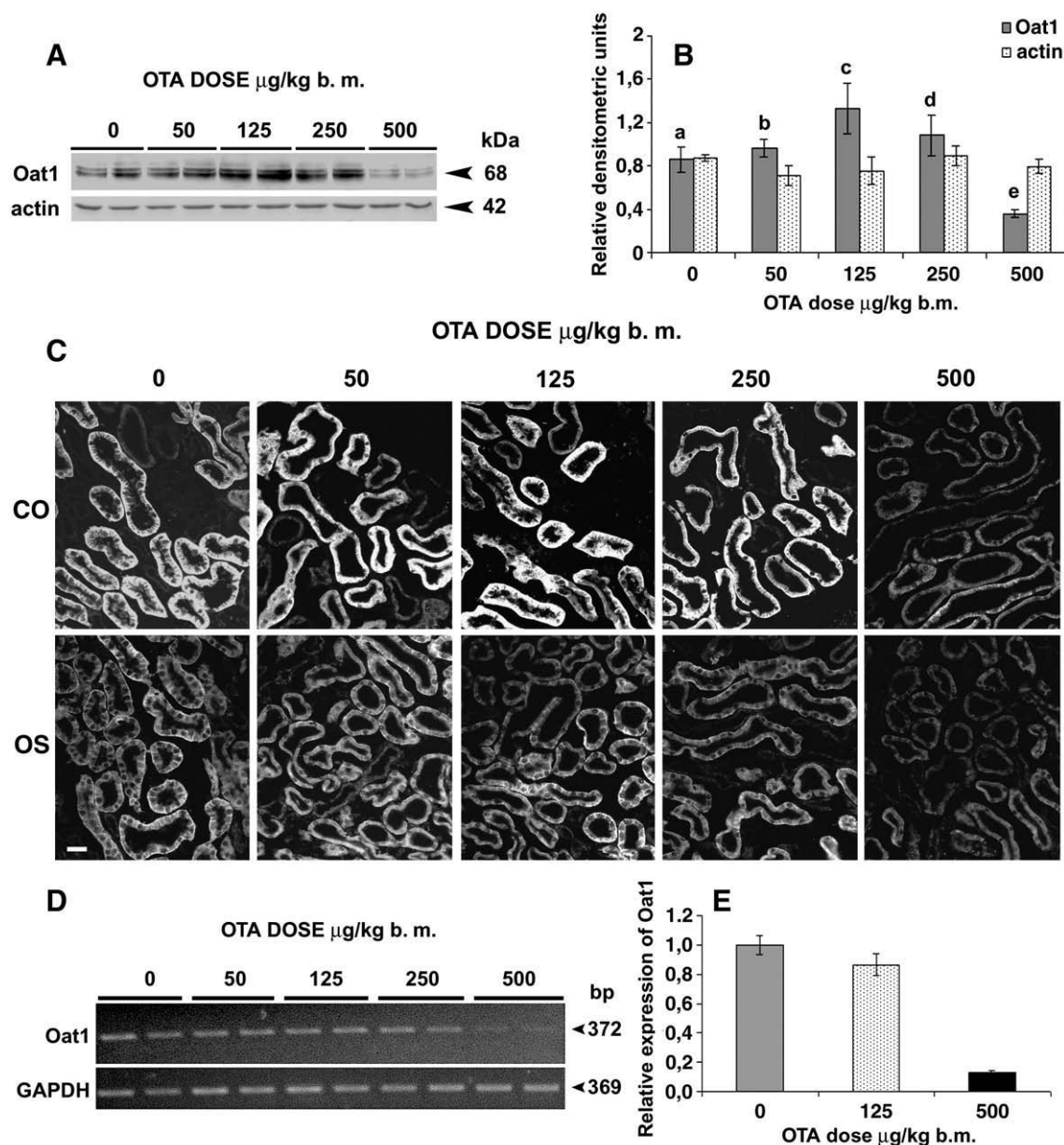


Fig. 4. rOat1 expression in rats treated with various doses of OTA. (A) Representative Western blots of rOat1 and α -actin proteins in TCM from the pooled kidney tissue (cortex plus outer stripe). (B) Densitometry of the protein bands is shown in A. Each bar is the mean \pm SE of the data from 4 independent TCM preparations. Versus the data in control rats (0), the abundance of rOat1 protein in isolated TCM increased \sim 50% at 125 μ g OTA/kg b.m. and decreased \sim 70% at 500 μ g OTA/kg b.m., respectively ($P < 0.05$: $c > a$, $e < a$, b, c, d). The abundance of α -actin remained unchanged at all OTA doses. (C) Representative immunostaining of rOat1 in cryosections of the kidney cortex (CO) and outer stripe (OS). rOat1 was localized to the BLM of PT S2 (strong staining in the CO) and S3 segments (weak staining in the OS). The staining intensity visibly increased in the CO of rats treated with 125 μ g OTA/kg b.m., and strongly diminished in both CO and OS of rats treated with 500 μ g OTA/kg b.m. Bar = 20 μ m. (D) The representative end-point RT-PCR data, performed with the independent cDNA preparations from two animals in each experimental group: the rOat1 mRNA expression was not visibly affected by up to 250 μ g OTA/kg b.m., and was strongly downregulated in rats treated with 500 μ g OTA/kg b.m. The expression of mRNA for housekeeping gene GAPDH remained unchanged in the animals treated with all OTA doses. (E) The representative real-time RT-PCR data are provided in duplicate measurements in cDNAs from two animals of each experimental group (mean \pm SE): the relative expression for Oat1 mRNA was unaffected by 125 μ g OTA/kg b.m., whereas the OTA dose of 500 μ g/kg b.m. strongly (\sim 85%) downregulated its expression.

In accordance with previous findings (Anzai et al., 2005; Kwak et al., 2005), the rOat5 protein was immunolocalized to the BBM and intracellular organelles of PT S3 segments in the outer stripe and medullary rays (c.f., Fig. 3D, and Fig. 7C). By Western blotting of TCM from the renal tissue, the protein was detected as the 72 kDa band (Fig. 7A). The immunoblot in A, and densitometric evaluation of the bands in B indicated an increased abundance of rOat5 protein in the membranes at OTA doses of 50–250 μ g/kg b.m. (up to \sim 150% above controls), whereas in rats treated with 500 μ g OTA/kg b.m., the protein abundance matched the control values. In tissue cryosections, the staining intensity and the number of stained tubules in the outer stripe increased in rats treated with OTA doses of 125 (not shown) and

250 μ g/kg b.m., while the staining at 500 μ g OTA/kg b.m. was similar to that in controls (C). The end-point (D) and real-time RT-PCR (E) studies showed no change in the rOat5 mRNA expression at 50–250 μ g OTA/kg b.m., and clear downregulation (\sim 50% vs. controls) at 500 μ g OTA/kg b.m.

OTA and parameters of oxidative stress in the renal tissue and urine

In order to test if the observed changes in the expression of various OTA-transporting Oats are associated with the tissue accumulation of OTA and oxidative stress, in the following experiment we measured OTA in the renal tissue and urine, and two

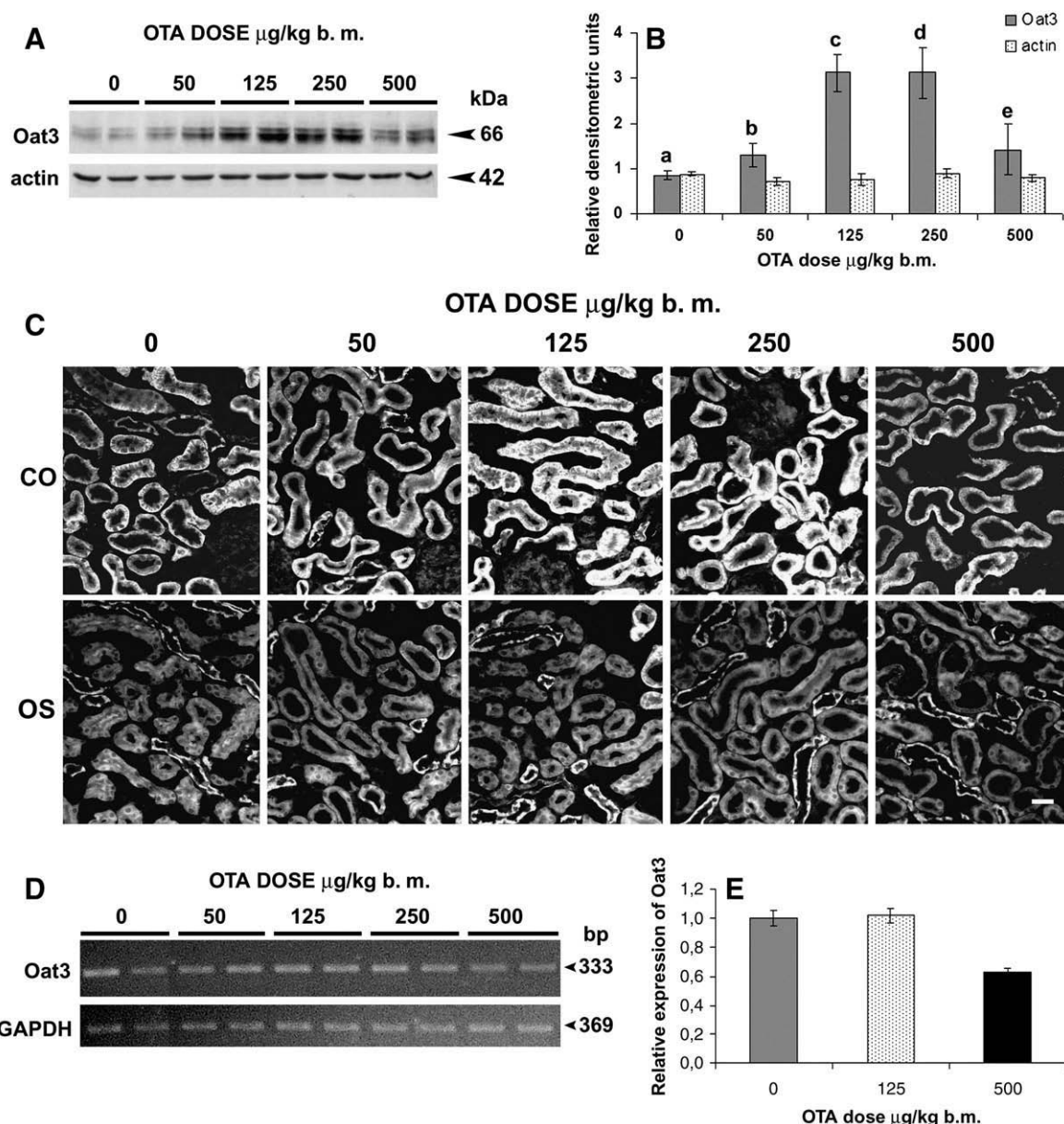


Fig. 5. rOat3 expression in rats treated with various doses of OTA. (A) Representative Western blots of rOat3 and α -actin proteins in TCM from the pooled kidney cortex and outer stripe tissue. (B) Densitometry of the protein bands shown in A. Each bar is the mean \pm SE of the data from 4 independent TCM preparations. The abundance of rOat3 protein in TCM increased with increasing OTA dose, reaching its maximum at 125–250 μ g OTA/kg b.m. (\sim 200% above controls; $P < 0.05$: $c > a, b, e$; $d > a, b, e$), and then decreased to about control levels at 500 μ g OTA/kg b.m. The abundance of α -actin remained unchanged in all OTA-treated groups. (C) Representative immunostaining of rOat3 in cryosections of the kidney cortex (CO) and outer stripe (OS): rOat3 was localized to the BLM in various nephron segments in these zones and in the inner stripe and inner medulla (data not shown; cf. Ljubojevic et al., 2004). In the CO tubules, the staining intensity was clearly stronger in rats treated with 125–250 μ g OTA/kg b.m., whereas at 500 μ g OTA/kg b.m., the staining intensity in the CO was similar to that in controls. In the tubules of OS, and inner medulla (not shown), the staining intensity remained unaffected by OTA treatment. Bar = 20 μ m. (D) Representative end-point RT-PCR data, performed with independent cDNA preparations from two animals in each experimental group, showed a largely unaffected expression of rOat3 mRNA by up to 250 μ g OTA/kg b.m., and partial downregulation at the highest OTA dose. The housekeeping gene GAPDH mRNA expression was not affected by any OTA dose. (E) Representative real-time RT-PCR data, are provided in duplicate measurements in cDNAs from two animals of each experimental group (mean \pm SE): the relative mRNA expression for rOat3 was unaffected by OTA dose of 125 μ g/kg b.m., and decreased (\sim 40% in respect to control) by OTA dose of 500 μ g/kg b.m.

parameters of oxidative stress, e.g., MDA in the renal tissue and urine and 8-OHdG in the urine of control (vehicle-treated) and OTA-treated rats. A lipid peroxidation product MDA, and an oxidative DNA adduct 8-OHdG, are the indicators of oxidative stress that can be measured in the affected tissue and/or urine (reviewed by Cooke et al., 2000 and Draper et al., 2000). The OTA treatment was performed with 250 or 500 μ g OTA/kg b.m., e.g., with doses that in the precedent studies resulted in upregulation and downregulation of the tested Oats, respectively. Where possible, the data before the treatment, as well as the comparable data in liver, were also provided.

The respective data are summarized in Table 2. Within the 10-day period, the treatment with both OTA doses did not affect the animal body mass, the kidney mass, and the volume of 24-h urine. Furthermore, control rats did not contain OTA in the renal tissue and urine. On the contrary, rats treated with 250 μ g OTA/kg b.m. exhibited a marked accumulation of this mycotoxin in the renal tissue and excretion in the urine, whereas in rats treated with 500 μ g OTA/kg b.m., the OTA accumulation in the renal tissue further increased 2.3-fold, and the OTA excretion in the urine further increased 3.9-fold. However, the levels of MDA were not increased neither in the renal tissue nor in urine, whereas the levels of 8-OHdG in the urine of both

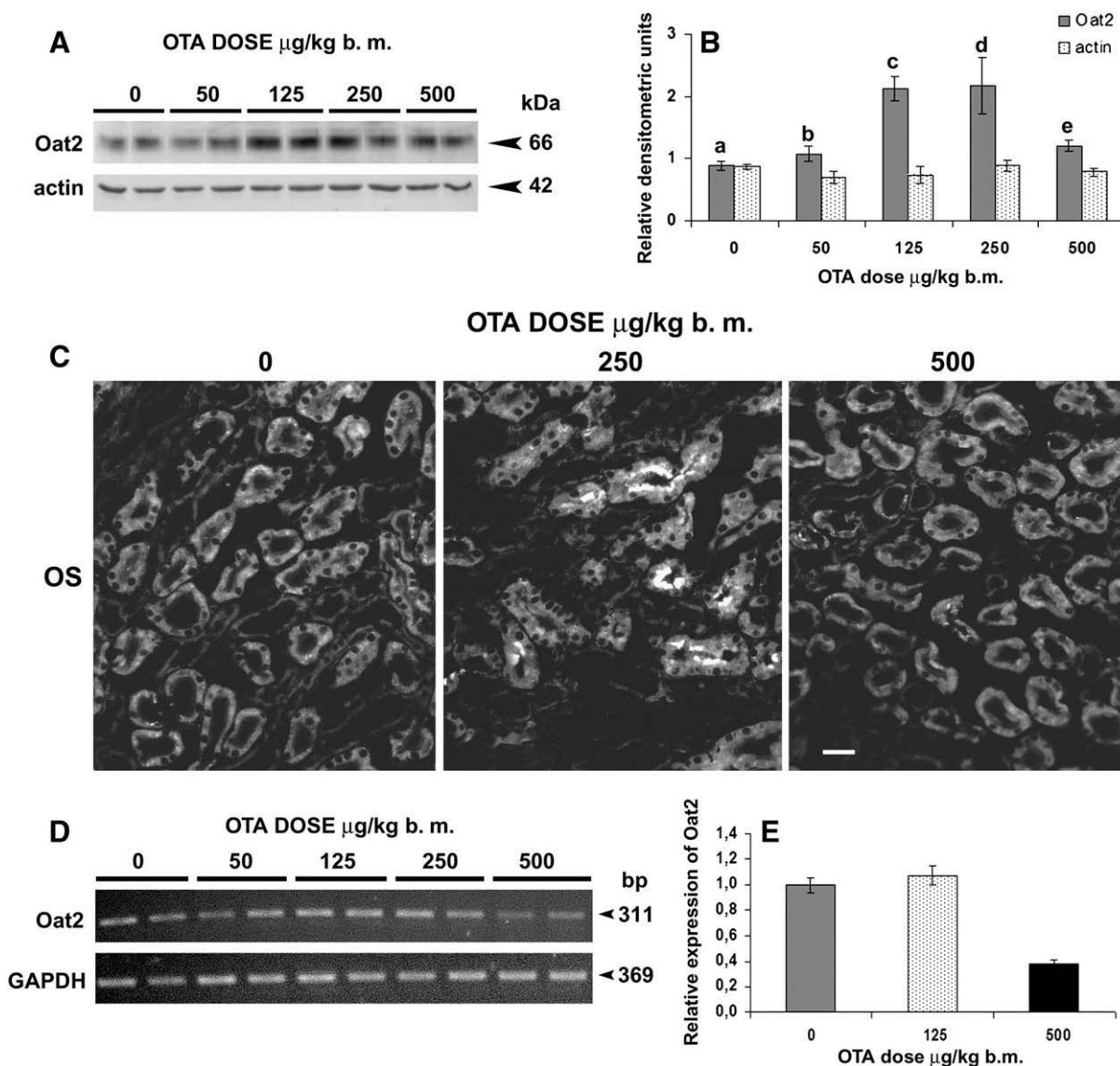


Fig. 6. rOat2 expression in rats treated with various doses of OTA. (A) Representative Western blots of rOat2 and α -actin proteins in TCM from the pooled kidney cortex and outer stripe tissue. (B) Densitometry of the protein bands shown in A. Each bar is the mean \pm SE of the data from 4 independent TCM preparations. The abundance of rOat2 protein in TCM increased with increasing the OTA dose, reaching maximum at 125–250 μ g OTA/kg b.m. (~140% above controls), and decreased to control levels at 500 μ g OTA/kg b.m. ($P < 0.05$: c > a, b, e; d > a, b, e). The abundance of α -actin remained unchanged in all OTA-treated groups. (C) Representative immunostaining of rOat2 in cryosections of the kidney outer stripe (OS), where rOat2 protein is localized in low abundance to the brush border of PT S3 segments (Ljubojevic et al., 2007). In control animals (0), most of the S3 segments were negative and occasional tubules were weakly apically positive. In animals treated with 125 (not shown) and 250 μ g OTA/kg b.m., more positive tubules with higher staining intensity were found in respect to controls. At OTA dose of 500 μ g/kg b.m., the immunostaining was negligible. Bar = 20 μ m. (D) Representative RT-PCR data are performed with independent cDNA preparations from two animals in each experimental group: rOat2 mRNA expression was similar at OTA doses of up to 250 μ g/kg b.m., and clearly diminished at 500 μ g OTA/kg b.m. The expression of mRNA for housekeeping gene GAPDH was unaffected in all OTA-treated rats. (E) Representative real-time RT-PCR data are provided in duplicate measurements in cDNAs from two animals of each experimental group (mean \pm SE), revealed that the relative mRNA expression for rOat2 was unaffected and strongly downregulated (~65% in respect to control) by OTA doses of 125 and 500 μ g/kg b.m., respectively.

vehicle-treated and OTA-treated rats were highly variable and similar, but 3–4-fold higher than the levels before the treatment. Therefore, the urine 8-OHdG seems to be elevated due to the treatment-related stress (gavage of the vehicle/OTA and/or collection of urine in the metabolic cages) and not due to the OTA-related oxidative stress in the renal tissue. Contrary to the situation in kidneys, the liver tissue of the same animals accumulated OTA in similar concentrations, but the MDA concentration increased moderately (~30%) in rats treated with 250 μ g OTA/kg b.m., and strongly (~100%) in rats treated with 500 μ g OTA/kg b.m. (Table 2). In additional experiments, in kidneys of these rats we have tested two other cellular parameters of oxidative stress (Sato and Bremner, 1993; Sabolic, 2006, and references therein), e.g., the concentration of glutathione (GSH) in the kidney tissue biochemically, and the expression of metallothionein in PT immuno-

cytochemically. The tissue concentration of GSH remained unaffected by both OTA doses (data not shown). The application of commercial monoclonal antibody against the horse metallothionein revealed in control rats a heterogeneous intensity of the cytoplasmic staining in PT cells; this staining pattern was not affected in rats treated with 50–250 μ g OTA/kg b.m., but in rats treated with 500 μ g OTA/kg b.m., the overall staining intensity was strongly diminished (data not shown).

Discussion

Previous studies in OTA-treated mice, rats and rabbits described alterations in renal function and structure induced with subchronic treatment with high doses (≥ 500 μ g/kg b.m./day, for 5–10 days) or with chronic treatment with lower doses (100–250 μ g/kg b.m./day,

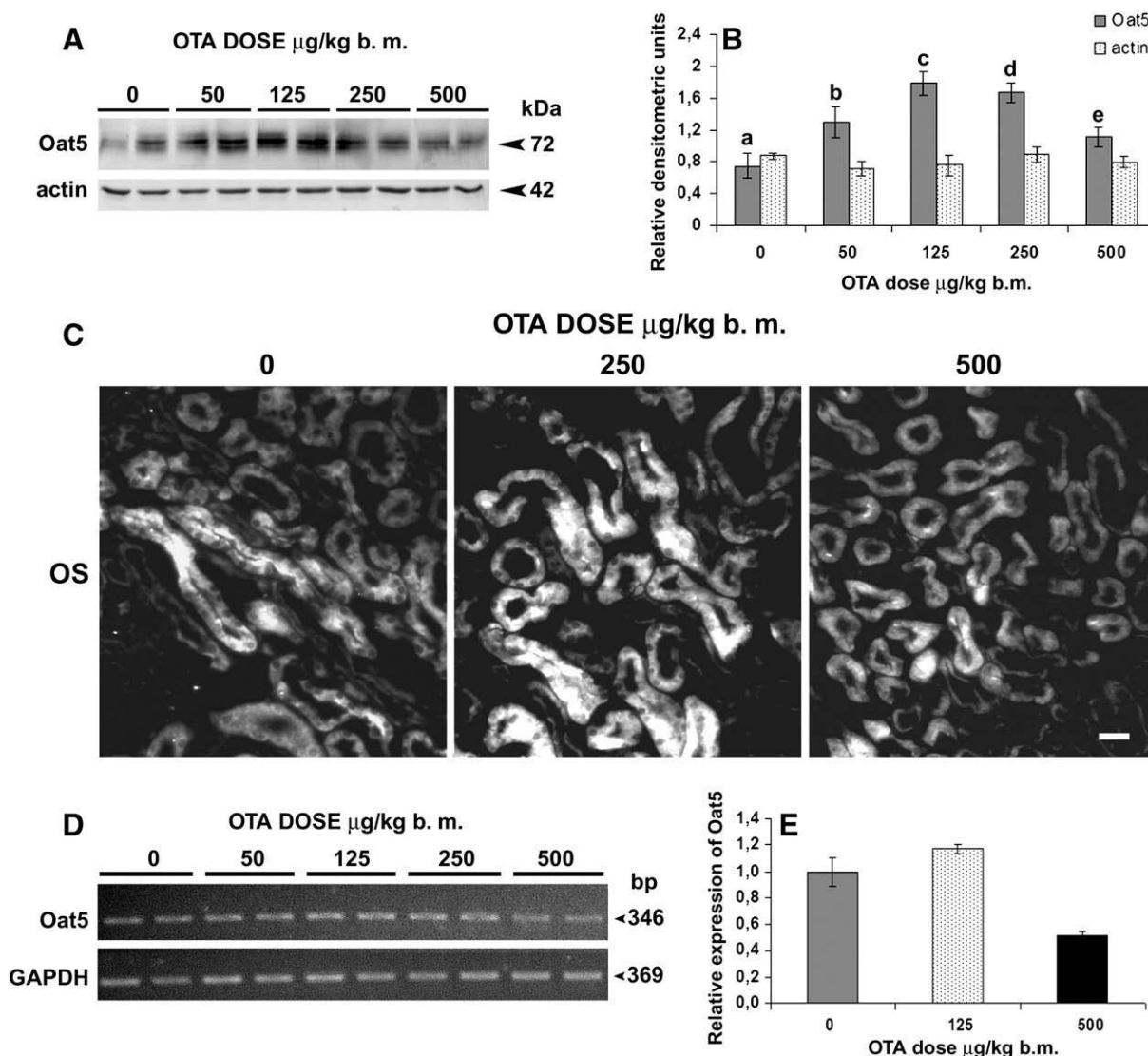


Fig. 7. rOat5 expression in rats treated with various doses of OTA. (A) Representative Western blots of rOat5 and α -actin proteins in TCM from the pooled kidney cortex and outer stripe tissue. (B) Densitometry of the protein bands shown in A. Each bar is the mean \pm SE of the data from 4 independent TCM preparations. The OTA doses of 50–250 $\mu\text{g}/\text{kg}$ b.m. significantly increased the abundance of rOat5 protein in TCM (up to \sim 150% above controls), whereas the dose of 500 $\mu\text{g}/\text{kg}$ OTA/kg b.m. had no effect compared with controls ($P < 0.05$: $b > a$; $c > a$, e ; $d > a$, e). The abundance of α -actin remained unchanged in TCM from all OTA-treated groups of rats. (C) Representative immunostaining of rOat5 in cryosections of the kidney outer stripe (OS). The staining was localized to the brush border and intracellular vesicles in the cells of PT S3 segments (c.f., Fig. 2D). The staining intensity and the number of positive tubules increased in rats treated with OTA doses of 125 (not shown) and 250 $\mu\text{g}/\text{kg}$ b.m., whereas the staining at OTA dose of 500 $\mu\text{g}/\text{kg}$ b.m. was similar to that in controls. Bar = 20 μm . (D) Representative RT-PCR data, performed with independent cDNA preparations from two animals in each experimental group: the expression of mRNA for rOat5 was unaffected by OTA doses of up to 250 $\mu\text{g}/\text{kg}$ b.m., and visibly diminished at the highest dose. The expression of GAPDH mRNA in all OTA-treated rats remained unchanged. (E) Representative real-time RT-PCR data are provided in duplicate measurements in cDNAs from two animals of each experimental group (mean \pm SE): the relative mRNA expression for rOat5 was unaffected and downregulated (\sim 50% in respect to control) by OTA doses of 125 and 500 $\mu\text{g}/\text{kg}$ b.m., respectively.

for a few weeks to two years) of this mycotoxin. These studies revealed only limited, OTA dose-dependent defects in renal reabsorptive and secretory functions, whereas the morphological damage was observed primarily in PT at high OTA doses applied for a longer time (Gekle et al., 1993; Gekle and Silbernagl, 1996; Kumar et al., 2007; Rached et al., 2007; Rasonyi et al., 1999). In the present study, we also did not observe major changes in the usual urinary parameters (urine volume, glucose, creatinine, protein, phosphate, potassium, chloride, and sodium), which remained largely unaffected even in rats treated with the highest OTA dose, thus indicating that, overall, the reabsorptive and secretory kidney functions in our rats were not significantly affected with OTA.

Our studies of tissue morphology and integrity of microtubules clearly revealed an OTA dose-dependent damage of epithelial cells, predominantly in the PT S3 segments located in the medullary rays. S3 segments in the outer stripe as well as the proximal convoluted

tubules and other nephron segments in the cortex and inner medulla exhibited no visible morphological damage. However, the upregulating effects upon rOats in all PT segments, as well as the damaging effect upon microtubule network in proximal and other tubules, indicate that the whole nephron underwent some OTA-related toxic influences. Our data support the findings by others, showing S3 segments in the medullary rays as the most sensitive nephron part to OTA in rats (Rached et al., 2007; Rasonyi et al., 1999). The studies in isolated microperfused tubules from rat kidneys indicated S3 as the site of highest reabsorption of OTA (Dahlmann et al., 1998), which may be mediated by the H^+ -dipeptide cotransporter (possibly PEPT2) and by several OA transporter (Oat2, Oat5, and OAT-K1) predominantly localized in the BBM of this PT segment (Anzai et al., 2005; Kwak et al., 2005; Ljubojevic et al., 2007; Masuda et al., 1997; Shen et al., 1999). The reason for such hypersensitivity of S3 cells in the medullary rays to OTA is not clear. These cells may have either the highly efficient

Table 2

Body and kidney mass, accumulation of OTA and MDA in the renal and liver tissues, and urine excretion of OTA, MDA, and 8-OHdG in rats before and after the 10-day treatment with vehicle (0) or two different doses of OTA.

OTA dose ($\mu\text{g}/\text{kg}$ b.m.)	Before the treatment	After the treatment		
	0	0	250	500
Body mass (g)	291 \pm 3.4	318 \pm 9.4	319 \pm 11.6	318 \pm 1.7
Kidney mass (mg) ^a	N.D.	1501 \pm 38	1599 \pm 40	1516 \pm 53
<i>Parameters in the renal tissue (cortex plus outer stripe)</i>				
OTA (ng/g tissue)	N.D.	0	40 \pm 7.0	92 \pm 4.8 ^b
MDA (nmol/g tissue)	N.D.	130 \pm 10.6	150 \pm 8.4	159 \pm 16.1
<i>Parameters in the liver tissue</i>				
OTA (ng/g tissue)	N.D.	0	52 \pm 8.5	112 \pm 18 ^b
MDA (nmol/g tissue)	N.D.	128 \pm 9.8	167 \pm 19.4	261 \pm 5.1 ^b
<i>Parameters in urine</i>				
Volume (mL/24 h)	24.7 \pm 2.86	26.0 \pm 2.83	24.5 \pm 2.21	23.8 \pm 3.35
OTA (ng/mL)	0	0	1.31 \pm 0.40	5.10 \pm 0.80 ^b
MDA ($\mu\text{mol}/\text{L}$)	0.81 \pm 0.15	0.78 \pm 0.20	0.40 \pm 0.10 ^c	0.41 \pm 0.13
($\mu\text{mol}/\text{g}$ creatinine)	1.05 \pm 0.24	1.59 \pm 0.43	0.71 \pm 0.18	0.60 \pm 0.15
8-OHdG (nmol/L)	85 \pm 28	266 \pm 67 ^c	225 \pm 57 ^c	200 \pm 53
(nmol/g creatinine)	115 \pm 43	514 \pm 111 ^c	422 \pm 139	376 \pm 125

Shown are the data (mean \pm SEM) measured in the tissue samples, and in urine before the treatment ($N = 12$ in each group) and after the 10-day treatment with indicated OTA doses ($N = 4$ in each experimental group). N.D., not determined.

^a Both kidneys.

^b Significantly different from the data obtained with 250 μg OTA/kg b.m.

^c Significantly different from the "before the treatment" data. Other comparisons are not significant.

mechanisms of OTA accumulation and/or highly inefficient mechanisms for its elimination, and/or a very low content of intracellular ROS scavengers and other molecules that could protect from the possible OTA-generated oxidative stress and damage. It is, however, interesting that in rats treated even with the highest OTA dose, a significant damage of S3 in the medullary rays did not disturb the urine parameters related to the kidney function, such as the volume, glucose, protein, creatinine and various ions. This indicates that either the respective part of S3 played an overall minor role in handling these parameters or that other, unaffected S3 segments in the outer stripe and the distal parts of the nephron compensated for the functional loss of the damaged S3 segment in the medullary rays.

The immunochemical and RT-PCR data show that the OTA treatment had a dose-dependent effect on the rOats abundance in the cell membrane and the expression of their mRNA in the renal tissue. In rats treated with lower OTA doses (≤ 250 $\mu\text{g}/\text{kg}$ b.m.) we observed an upregulation of the tested rOat proteins without a change in their mRNA expression. The unchanged expression of rOats mRNA indicates an involvement of post-transcriptional, stimulatory effects of low OTA doses on the transporter abundances. Previous short-term studies have identified a number of compounds and some peptide hormones that stimulated or inhibited the OA transport and/or changed the activity of relevant Oats in various experimental models *in vitro* and *in vivo* (reviewed in Terlouw et al., 2003). These effects, however, occurred within a few minutes to a few hours through protein kinase-mediated intracellular signaling which involved changing in phosphorylation of the transporters and/or exocytotic recruitment of dormant transporters from an intracellular storage compartment. These mechanisms are not expected to change the total abundance of a transporter in the cell/isolated TCM, and thus are unlikely cause of the enhanced abundance of four renal rOats in our rats treated with low OTA doses. On the other side, the long-term regulation of expression of rat renal rOat1 and rOat3 proteins is driven by strong androgen stimulation and weak estrogen inhibition at their mRNA level (Buist et al., 2002; Ljubojevic et al., 2004), whereas the expression of rOat2 and rOat5 proteins is regulated by strong androgen inhibition and weak estrogen stimulation, also at their

mRNA level (Ljubojevic et al., 2007; Sabolic et al., 2007, and references there in). Since these hormones have completely different effects on the transporters in opposite membrane domains, the low OTA dose-induced upregulation of both basolateral and apical rOats can not be mediated by the levels of sex hormones. We, however, cannot exclude the possibility that low doses of OTA affected the levels of thyroid hormones and/or glucocorticoids, which were previously shown to stimulate the rOat1-mediated PAH uptake in the renal cortical slices from rats treated with these hormones (Bahn et al., 2003; Terlouw et al., 2003). Since OTA is a substrate for all four rOats, their higher expression driven by low OTA doses may represent a phenomenon of substrate-induced stimulation, similar to that observed for rOat1 after 7-day administration of loop diuretics in rats (Kim et al., 2003), which may result from a post-transcriptional increased synthesis and/or decreased degradation of rOat proteins.

The highest OTA dose (500 $\mu\text{g}/\text{kg}$ b.m.) affected the expression of rOats at the level of both protein and mRNA. However, at the level of protein in isolated TCM, only the rOat1 abundance decreased below the control values ($\sim 70\%$). Considering strong upregulation of all four rOats with the OTA doses of 125–250 $\mu\text{g}/\text{kg}$ b.m., the lower (albeit control) levels of protein abundances in rats treated with the highest OTA dose point to an active downregulating process, which is supported by RT-PCR data showing diminished expression of mRNA for all four rOats. mRNA for the housekeeping gene GAPDH was not affected by any OTA dose, indicating that OTA was not generally toxic but exhibited some specificity in targeting. Diminished expression of rOat1 protein in PT in rats treated with the highest OTA dose may explain the previously observed OTA-induced reduction of PAH transport in the mammalian kidney *in vivo* and *in vitro* (Friis et al., 1988; Gekle and Silbernagl, 1994; Groves et al., 1998, 1999; Sauvart et al., 1998; Welborn et al., 1998). Having the highest affinity for PAH, rOat1 was recently described as a major contributor to the renal PAH transport/secretion in physiological and toxic conditions in rats (Habu et al., 2003), rabbits (Zhang et al., 2004), mice (Eraly et al., 2006) and humans (Nozaki et al., 2007), whereas Oat3 and Oats in the PT BBM play a relatively minor role in this process. Based on the down-regulating pattern of mRNA expression for other Oats with the highest OTA dose, one can assume that with longer treatment (> 10 days) with the highest OTA dose, the abundances of all rOat proteins in PT would further decrease and thus contribute to the loss of renal capacity in PAH secretion. However, our finding of a dramatic accumulation of OTA in the renal tissue in rats treated with 250, and even more so with 500 $\mu\text{g}/\text{kg}$ b.m., indicates that the previously observed impaired PAH accumulation in the renal cortical slices, and excretion *via* urine, may have two reasons: a) following subchronic treatment with low OTA doses, the accumulated OTA may directly interact with, and inhibit transport/secretion of PAH and other OA, and b) following chronic treatment with low OTA doses, or subchronic treatment with high OTA doses, the PAH transport may be inhibited by concerted action of accumulated OTA in the cells, lower expression of Oats in the respective membrane domains of PT, and loss of secretory and/or reabsorptive surface in the damaged epithelial cells.

An increased abundance of the renal OTA-transporting Oats in rats treated with low OTA doses (≤ 250 $\mu\text{g}/\text{kg}$ b.m.) may have wider pathophysiological meaning. Previous *in vivo* and *in vitro* studies have shown fair correlation between the expression level of various Oats and the transport rate of relevant OA (Bahn et al., 2003; Habu et al., 2003; Sabolic et al., 2007, and references there in; Schneider et al., 2007; Zhang et al., 2004). One can thus assume that the simultaneous upregulation of both basolateral (rOat1, rOat3) and apical (rOat2, rOat5) OTA transporters in the PT, as found in our rats treated with low OTA doses, may contribute to development of OTA nephrotoxicity with possibly the following pattern: a) the enhanced expression of rOat1 and rOat3 proteins may accelerate the intracellular OTA uptake *via* the BLM, whereas the enhanced expression rOat2 and rOat5 proteins may accelerate the OTA

reabsorption via the BBM, b) the accumulated OTA may directly interfere with the cellular handling of endogenous non-toxic and toxic OA, and impair their elimination by secretion into urine, and c) the accumulated both OTA and toxic OA may damage various intracellular structures/organelles directly and/or inhibit mitochondrial oxidative phosphorylation, decreasing production of ATP (Jung and Endou, 1989) and increasing generation of ROS, with further toxic consequences related to ROS. However, the levels of the well known indicators of oxidative stress, e.g., MDA, GSH, and 8-OHdG in the kidney tissue and/or urine of our rats treated with 250–500 µg OTA/kg b.m. did not change. The insensitivity of the applied methods was not the problem; the same methods detected a significant OTA dose-dependent increase in MDA in the liver tissue. Furthermore, low OTA doses (≤ 250 mg/kg b.m.) did not affect the expression of metallothionein in PT, but the dose of 500 mg/kg b.m. strongly downregulated it, indicating an unspecific, general toxicity of the high OTA dose in PT cells. However, a limited dose-dependent toxicity of OTA in other parts of the nephron, and particularly in the S3 segment, was demonstrated by the deranged structure and loss of the oxidative stress-sensitive microtubules. Therefore, most of our findings do not support the view that the accumulated OTA had a significant effect in generating oxidative stress in PT cells. Rather, the accumulated OTA may have directly affected the rOats expression at the mRNA and/or protein level, and damaged the cell cytoskeleton and morphology. Alternatively, MDA, GSH, metallothionein, and 8-OHdG may have been insensitive indicators of a limited oxidative stress in the kidney tissue.

Conflict of interest statement

The authors declare no conflict of interest regarding this collaborative work.

Acknowledgments

The authors acknowledge the expert technical assistance by Eva Heršak, Mirjana Matašin and Jasna Mileković. This study was approved by the Ethical Committee of the Institute for Medical Research and Occupational Health in Zagreb. The funding was provided by grants No. 022-0222148-2142 (M. Peraica) and 022-0222148-2146 (I. Sabolic) from the Ministry of Science, Education and Sports, Republic of Croatia.

Appendix A. Supplementary data

Supplementary data associated with this article can be found, in the online version, at doi:10.1016/j.taap.2009.06.008.

References

- Anzai, N., Jutabha, P., Enomoto, A., Yokoyama, H., Nonoguchi, H., Hirata, T., Shiraya, K., He, X., Seok, H.C., Takeda, M., Miyazaki, H., Sakata, T., Tomita, K., Igarashi, T., Kanai, Y., Endou, H., 2005. Functional characterization of rat organic anion transporter 5 (Slc22a19) at the apical membrane of renal proximal tubules. *J. Pharmacol. Exp. Ther.* 315, 534–544.
- Babu, E., Takeda, M., Narikawa, S., Kobayashi, Y., Enomoto, A., Tojo, A., Cha, S.H., Sekine, T., Sakthisekaran, D., Endou, H., 2002. Role of human organic anion transporter 4 in the transport of ochratoxin A. *Biochim. Biophys. Acta* 1590, 64–75.
- Bahn, A., Hauss, A., Appenroth, D., Ebbinghaus, D., Hagos, Y., Steinmetzer, P., Burckhardt, G., Fleck, C., 2003. RT-PCR-based evidence for the in vivo stimulation of renal tubular p-aminohippurate (PAH) transport by triiodothyronine (T3) or dexamethasone (DEXA) in kidney tissue of immature and adult rats. *Exp. Toxicol. Pathol.* 54, 367–373.
- Bahnemann, E., Kerling, H.P., Ensminger, S., Schwerdt, G., Silbernagl, S., Gekle, M., 1997. Renal transepithelial secretion of ochratoxin A in the non-filtering toad kidney. *Toxicology* 120, 11–17.
- Bauer von, J., Gareis, M., Gedek, B., 1984. Zum Nachweis und Vorkommen von Ochratoxin A bei Schlachtschweinen. *Berl. Münch. Tierärztl. Wschr.* 97, 279–283.
- Boorman, G.A., McDonald, M.R., Imoto, S., Persing, R., 1992. Renal lesions induced by ochratoxin A exposure in the F344 rat. *Toxicol. Pathol.* 20, 236–245.
- Bradford, M.M., 1976. A rapid and sensitive method for the quantitation of microgram quantities of protein utilizing the principle of protein dye binding. *Anal. Biochem.* 72, 248–254.
- Breitholtz-Emanuelsson, A., Olsen, M., Oskarsson, A., Palminger, I., Hult, K., 1993. Ochratoxin A in cow's milk and in human milk with corresponding human blood samples. *J. AOAC Int.* 76, 842–846.
- Buist, S.C.N., Cherrington, N.J., Choudhuri, S., Hartley, D.P., Klaassen, C.D., 2002. Gender-specific and developmental influences on the expression of rat organic anion transporters. *J. Pharmacol. Exp. Ther.* 301, 145–151.
- Castegnaro, M., Mohr, U., Pfuhl-Leskowicz, A., Estève, J., Steinmann, J., Tillmann, T., Michelon, J., Bartsch, H., 1998. Sex- and strain-specific induction of renal tumors by ochratoxin A in rats correlates with DNA adduction. *Int. J. Cancer Suppl.* 77, 70–75.
- Cavin, C., Delatour, T., Marin-Kuan, M., Holzhäuser, D., Higgins, L., Bezençon, C., Guignard, G., Junod, S., Richoz-Payot, J., Gremaud, E., Hayes, J.D., Nestler, S., Mantle, P., Schilter, B., 2007. Reduction in antioxidant defenses may contribute to ochratoxin A toxicity and carcinogenicity. *Toxicol. Sci.* 96, 30–39.
- Cha, S.H., Sekine, T., Fukushima, J.I., Kanai, Y., Kobayashi, Y., Goya, T., Endou, H., 2001. Identification and characterization of human organic anion transporter 3 expressing predominantly in the kidney. *Mol. Pharmacol.* 59, 1277–1286.
- Cooke, M.S., Evans, M.D., Herbert, K.E., Lunec, J., 2000. Urinary 8-hydroxy-2'-deoxyguanosine – source, significance and supplements. *Free Radic. Res.* 32, 381–397.
- Dahlmann, A., Dantzer, W.H., Silbernagl, S., Gekle, M., 1998. Detailed mapping of ochratoxin A reabsorption along the rat nephron in vivo: the nephrotoxin can be reabsorbed in all nephron segments by different mechanisms. *J. Pharmacol. Exp. Ther.* 286, 157–162.
- Domijan, A.-M., Peraica, M., 2008. Determination of 8-hydroxyguanosine in urine using HPLC with electrochemical detection. *Arh. Hig. Rada. Toksikol.* 59, 181–277.
- Draper, H.H., Csallany, A.S., Hadley, M., 2000. Urinary aldehydes as indicators of lipid peroxidation in vivo. *Free Radic. Biol. Med.* 29, 1071–1077.
- Drury, J.A., Nycyk, J.A., Cooke, R.W.I., 1997. Comparison of urinary and plasma malondialdehyde in preterm infants. *Clin. Chim. Acta* 263, 177–185.
- EFSA, 2006. Opinion of the Scientific Panel on contaminants in the food chain on a request from the commission related to ochratoxin A in food. Question number: EFSA-Q-2005-154. *EFSA Journal* 1–56.
- Enomoto, A., Takeda, M., Shimoda, M., Narikawa, S., Kobayashi, Y., Kobayashi, Y., Yamamoto, T., Sekine, T., Cha, S.H., Niwa, T., Endou, H., 2002. Interaction of human organic anion transporters 2 and 4 with organic anion transport inhibitors. *J. Pharmacol. Exp. Ther.* 301, 797–802.
- Eraly, S.A., Vallon, V., Vaughan, D.A., Gangotri, J.A., Richter, K., Nagle, M., Monte, J.C., Rieg, T., Truong, D.M., Long, J.M., Barshop, B.A., Kaler, G., Nigam, S.K., 2006. Decreased renal organic anion secretion and plasma accumulation of endogenous organic anions in OAT1 knock-out mice. *J. Biol. Chem.* 281, 5072–5083.
- Friis, C., Brinn, R., Hald, B., 1988. Uptake of ochratoxin A by slices of pig kidney cortex. *Toxicology* 52, 209–217.
- Fuchs, R., Hult, K., 1992. Ochratoxin A in blood and its pharmacokinetic properties. *Food Chem. Toxicol.* 30, 201–204.
- Gekle, M., Silbernagl, S., 1994. The role of the proximal tubule in ochratoxin A nephrotoxicity in vivo: toxodynamic and toxokinetic aspects. *Ren. Physiol. Biochem.* 17, 40–49.
- Gekle, M., Silbernagl, S., 1996. Renal toxicodynamics of ochratoxin A: a pathophysiological approach. *Kidney Blood Press. Res.* 19, 225–235.
- Gekle, M., Oberleithner, H., Silbernagl, S., 1993. Ochratoxin A impairs “postproximal” nephron function in vivo and blocks plasma membrane anion conductance in Madin-Darby canine kidney cells in vitro. *Pflügers Arch.* 425, 401–408.
- Grosse, Y., Chekir-Ghedira, L., Huc, A., Obrecht-Pflumio, S., Dirheimer, G., Bacha, H., Pfohl-Leskowicz, A., 1997. Retinol, ascorbic acid and α -tocopherol prevent DNA adduct formation in mice treated with the mycotoxins ochratoxin A and zearalenone. *Cancer Lett.* 114, 225–229.
- Groves, C.E., Morales, M., Wright, S.H., 1998. Peritubular transport of ochratoxin A in rabbit renal proximal tubules. *J. Pharmacol. Exp. Ther.* 284, 943–948.
- Groves, C.E., Nowak, G., Morales, M., 1999. Ochratoxin A secretion in primary cultures of rabbit renal proximal tubule cells. *J. Am. Soc. Nephrol.* 10, 13–20.
- Habu, Y., Yano, I., Takeuchi, A., Saito, H., Okuda, M., Fukatsu, A., Inui, K.I., 2003. Decreased activity of basolateral organic ion transporters in hyperuricemic rat kidney: roles of organic ion transporters, rOAT1, rOAT3 and rOCT2. *Biochem. Pharmacol.* 66, 1107–1114.
- Jung, K.Y., Endou, H., 1989. Nephrotoxicity assessment by measuring cellular ATP content. II. Intranephron site of ochratoxin A nephrotoxicity. *Toxicol. Appl. Pharmacol.* 100, 383–390.
- Jung, K.Y., Takeda, M., Kim, D.K., Tojo, A., Narikawa, S., Yoo, B.S., Hosoyamada, M., Cha, S.H., Sekine, T., Endou, H., 2001. Characterization of ochratoxin A transport by human organic anion transporters. *Life Sci.* 69, 2123–2135.
- Kamp, H.G., Eisenbrand, G., Janzowski, C., Kiossev, J., Latendresse, J.R., Schlatter, J., Turesky, R.J., 2005. Ochratoxin A induces oxidative DNA damage in liver and kidney after oral dosing to rats. *Mol. Nutr. Food Res.* 49, 1160–1167.
- Kim, G.H., Na, K.Y., Kim, S.Y., Joo, K.W., Oh, Y.K., Chae, S.W., Endou, H., Han, J.S., 2003. Up-regulation of organic anion transporter 1 protein is induced by chronic furosemide or hydrochlorothiazide infusion in rat kidney. *Nephrol. Dial. Transplant.* 18, 1505–1511.
- Kobayashi, Y., Ohshiro, N., Shibusawa, A., Sasaki, T., Tokuyama, S., Sekine, T., Endou, H., Yamamoto, T., 2002. Isolation, characterization and differential gene expression of multispecific organic anion transporter 2 in mice. *Mol. Pharmacol.* 62, 7–14.
- Kojima, R., Sekine, T., Kawachi, M., Seok, H.C., Suzuki, Y., Endou, H., 2002. Immunolocalization of multispecific organic anion transporters, OAT1, OAT2, and OAT3, in rat kidney. *J. Am. Soc. Nephrol.* 13, 848–857.
- Kuiper-Goodman, T., Scott, P.M., 1989. Risk assessment of the mycotoxin ochratoxin A. *Biomed. Environ. Sci.* 2, 179–248.

- Kumar, M., Dwivedi, P., Sharma, A.K., Singh, N.D., Patil, R.D., 2007. Ochratoxin A and citrinin nephrotoxicity in New Zealand White rabbits: an ultrastructural assessment. *Mycopathologia* 163, 21–30.
- Kusuhara, H., Sekine, T., Utsunomiya-Tate, N., Tsuda, M., Kojima, R., Cha, S.H., Sugiyama, Y., Kanai, Y., Endou, H., 1999. Molecular cloning and characterization of a new multispecific organic anion transporter from rat brain. *J. Biol. Chem.* 274, 13675–13680.
- Kwak, J.O., Kim, H.W., Oh, K.J., Ko, C.B., Park, H., Cha, S.H., 2005. Characterization of mouse organic anion transporter 5 as a renal steroid sulfate transporter. *J. Steroid Biochem. Mol. Biol.* 97, 369–375.
- Lee, S.C., Beery, J.T., Chu, F.S., 1984. Immunohistochemical fate of ochratoxin A in mice. *Toxicol. Appl. Pharmacol.* 72, 218–227.
- Leier, I., Hummel-Eisenbeiss, J., Cui, Y., Keppler, D., 2000. ATP-dependent para-aminohippurate transport by apical multidrug resistance protein MRP2. *Kidney Int.* 57, 1636–1642.
- Ljubojevic, M., Herak-Kramberger, C.M., Hagos, Y., Bahn, A., Endou, H., Burckhardt, G., Sabolic, I., 2004. Rat renal cortical OAT1 and OAT3 exhibit gender differences determined by both androgen stimulation and estrogen inhibition. *Am. J. Physiol. Renal. Physiol.* 287, F124–F138.
- Ljubojevic, M., Balen, D., Breljak, D., Kusan, M., Anzai, N., Bahn, A., Burckhardt, G., Sabolic, I., 2007. Renal expression of organic anion transporter OAT2 in rats and mice is regulated by sex hormones. *Am. J. Physiol. Renal. Physiol.* 292, F361–F372.
- Masuda, S., Saito, H., Nonoguchi, H., Tomita, K., Inui, K.I., 1997. mRNA distribution and membrane localization of the OAT-K1 organic anion transporter in rat renal tubules. *FEBS Lett.* 407, 127–131.
- Nozaki, Y., Kusuhara, H., Kondo, T., Hasegawa, M., Shiroyanagi, Y., Nakazawa, H., Okano, T., Sugiyama, Y., 2007. Characterization of the uptake of organic anion transporter (OAT) 1 and OAT3 substrates by human kidney slices. *J. Pharmacol. Exp. Ther.* 321, 362–369.
- Ohkawa, H., Ohishi, N., Yagi, K., 1979. Assay for lipid peroxides in animal tissue by thiobarbituric acid reaction. *Analyt. Biochem.* 95, 351–358.
- Petrik, J., Zanic-Grubisic, T., Barisic, K., Pepeljnjak, S., Radic, B., Ferencic, Z., Cepelak, I., 2003. Apoptosis and oxidative stress induced by ochratoxin A in rat kidney. *Arch. Toxicol.* 77, 685–693.
- Pfohl-Leszkowicz, A., Manderville, R.A., 2007. Ochratoxin A: an overview on toxicity and carcinogenicity in animals and humans. *Mol. Nutr. Food Res.* 51, 61–99.
- Rached, E., Hard, G.C., Blumbach, K., Weber, K., Draheim, R., Lutz, W.K., Ozden, S., Steger, U., Dekant, W., Mally, A., 2007. Ochratoxin A: 13-week oral toxicity and cell proliferation in male F344/N rats. *Toxicol. Sci.* 97, 288–298.
- Rasonyi, T., Schlatter, J., Dietrich, D.R., 1999. The role of α 2u-globulin in ochratoxin A induced renal toxicity and tumors in F344 rats. *Toxicol. Lett.* 104, 83–92.
- Ringot, D., Chango, A., Schneider, Y.J., Larondelle, Y., 2006. Toxicokinetics and toxicodynamics of ochratoxin A, an update. *Chem. Biol. Interact.* 159, 18–46.
- Sabolic, I., 2006. Common mechanisms in nephropathy induced by toxic metals. *Nephron. Physiol.* 104, 107–114.
- Sabolic, I., Herak-Kramberger, C.M., Antolovic, R., Breton, S., Brown, D., 2006. Loss of basolateral invaginations in proximal tubules of cadmium-intoxicated rats is independent on microtubules and clathrin. *Toxicology* 218, 149–163.
- Sabolic, I., Asif, A., Budach, W., Wanke, C., Bahn, A., Burckhardt, G., 2007. Gender differences in kidney function. *Pflügers Arch. - Eur. J. Physiol.* 455, 397–429.
- Sato, M., Bremner, I., 1993. Oxygen free radicals and metallothionein. *Free Radicals Biol. Med.* 14, 325–337.
- Sauvant, C., Silbernagl, S., Gekle, M., 1998. Exposure to ochratoxin A impairs organic anion transport in proximal-tubule-derived opossum kidney cells. *J. Pharmacol. Exp. Ther.* 287, 13–20.
- Sauvant, C., Holzinger, H., Gekle, M., 2005. The nephrotoxin ochratoxin A induces key parameters of chronic interstitial nephropathy in renal proximal tubular cells. *Cell Physiol. Biochem.* 15, 125–134.
- Schaaf, G.J., Nijmeijer, S.M., Maas, R.F.M., Roestenberg, P., De Groene, E.M., Fink-Gremmels, J., 2002. The role of oxidative stress in the ochratoxin A-mediated toxicity in proximal tubular cells. *Biochim. Biophys. Acta* 1588, 149–158.
- Schneider, R., Sauvant, C., Betz, B., Otremba, M., Fischer, D., Holzinger, H., Wanner, C., Galle, J., Gekle, M., 2007. Downregulation of organic anion transporters OAT1 and OAT3 correlates with impaired secretion of para-aminohippurate after ischemic acute renal failure in rats. *Am. J. Physiol. Renal. Physiol.* 292, F1599–F1605.
- Shen, H., Smith, D.E., Yang, T., Huang, Y.G., Schneemann, J.B., Brosius 3rd, F.C., 1999. Localization of PEPT1 and PEPT2 proton-coupled oligopeptide transporter mRNA and protein in rat kidney. *Am. J. Physiol. Renal. Physiol.* 276, F658–F665.
- Sokol, P.P., Ripich, G., Holohan, P.D., Ross, C.R., 1988. Mechanism of ochratoxin A transport in kidney. *J. Pharmacol. Exp. Ther.* 246, 460–465.
- Takeuchi, A., Masuda, S., Saito, H., Abe, T., Inui, K.I., 2001. Multispecific substrate recognition of kidney-specific organic anion transporters OAT-K1 and OAT-K2. *J. Pharmacol. Exp. Ther.* 299, 261–267.
- Terlouw, S.A., Masereeuw, R., Russel, F.G.M., 2003. Modulatory effects of hormones, drugs, and toxic events on renal organic anion transport. *Biochem. Pharmacol.* 65, 1393–1405.
- Tsuda, M., Sekine, T., Takeda, M., Cha, S.H., Kanai, Y., Kimura, M., Endou, H., 1999. Transport of ochratoxin A by renal multispecific organic anion transporter 1. *J. Pharmacol. Exp. Ther.* 289, 1301–1305.
- Welborn, J.R., Groves, C.E., Wright, S.H., 1998. Peritubular transport of ochratoxin A by single rabbit renal proximal tubules. *J. Am. Soc. Nephrol.* 9, 1973–1982.
- Youngblood, G.L., Sweet, D.H., 2004. Identification and functional assessment of the novel murine organic anion transporter Oat5 (Slc22a19) expressed in kidney. *Am. J. Physiol. Renal. Physiol.* 287, F236–F244.
- Zhang, X., Groves, C.E., Bahn, A., Barendt, W.M., Prado, M.D., Rodiger, M., Chatsudhithong, V., Burckhardt, G., Wright, S.H., 2004. Relative contribution of OAT and OCT transporters to organic electrolyte transport in rabbit proximal tubule. *Am. J. Physiol. Renal. Physiol.* 287, F999–F1010.
- Zingerle, M., Silbernagl, S., Gekle, M., 1997. Reabsorption of the nephrotoxin ochratoxin A along the rat nephron in vivo. *J. Pharmacol. Exp. Ther.* 280, 220–224.